AIMS Mathematics

http://www.aimspress.com/journal/Math

AIMS Mathematics, 6(12): 13464–13479.
DOI: 10.3934/math.2021780
Received: 19 July 2021
Accepted: 06 September 2021
Published: 18 September 2021

Research article

Powell-Eyring fluid flow over a stratified sheet through porous medium with thermal radiation and viscous dissipation

W. Abbas[1] **and Ahmed M. Megahed**[2,*]

[1] Basic and Applied Science Department, College of Engineering and Technology, Arab Academy for Science, Technology and Maritime Transport, Cairo, Egypt

[2] Department of Mathematics, Faculty of Science, Benha University, Benha, Egypt

* **Correspondence:** Email: ahmed.abdelbaqk@fsc.bu.edu.eg; Tel: +201141387632.

Abstract: The present study explores the effects of viscous dissipation, the thermal dependent conductivity and the thermal dependent viscosity on the steady motion of a Powell-Eyring fluid over a stratified stretching sheet which embedded in a porous medium. The fact that the nature of non-Newtonian flows problems are highly nonlinear equations has been taken into consideration here and this was the motive objective to determine numerical solutions. So, the emphasis is on the methodology adopted for obtaining numerical solutions that yielded after employing the Chebyshev spectral method. The temperature distributions and the velocity components are evaluated by solving numerically the boundary value problems that correspond to the proposed problem. Then, some figures have been plotted to elucidates the effect of different physical parameters appearing in the problem on both the temperature and the velocity profiles. The presence of the thermal radiation and the viscous dissipation in the fluid flow are shown to have quite a dramatic effect on the temperature profiles. In culmination, cooling process in nuclear reactors and geothermal engineering especially in the presence of thermal stratification phenomenon can be adopted as an application of this study. The theoretical and the observed results provide a fairly good qualitative agreement.

Keywords: Eyring-Powell fluid; thermal stratification; chebyshev spectral method; thermal radiation; porous medium
Mathematics Subject Classification: 65L10, 76A05, 76D50, 76S05

Nomenclature

a The linear stretching rate
b_1 Dimensional constant
b_2 Dimensional constant
c_p The specific heat at constant pressure

f The dimensionless stream function
k^* The absorption coefficient
q_r The radiation heat flux
T The fluid temperature
T_0 The reference temperature
T_w The sheet temperature
T_∞ The temperature far away from the plate
u The velocity components along x direction
U_w The sheet velocity
v The velocity components along y direction

Greek symbols
ρ The density of the fluid
μ The viscosity of the fluid
ν Kinematic viscosity of the fluid
κ The fluid thermal conductivity
ψ Stream function
η Similarity variable
θ Dimensionless temperature
σ^* The Stefan-Boltzman constant
ε The thermal conductivity parameter

Subscripts
∞ free stream condition
w condition at the surface

1. Introduction

Investigation of the fluid flow characteristics and heat transfer due to stretched surfaces has gained considerable interest by the researchers owing to increase in the implementations in different applications of technology and science like condensation process, lubricants, fiber production, textiles machines plastic sheets and food processing, and etc. After a pioneering work by Crane [1], the problem of flow and heat transfer past stretched sheets with different situations and models has drawn considerable attention of literature has been generated on this problem. Chen [2] studied numerically the boundary layers laminar mixed convection flow past vertical stretching sheet with considering the velocity and temperature of the sheet vary in a power law form. Influence of chemical reaction on heat transfer and unsteady free convective over a stretching surface in a porous medium was studied by Chamkha and Mansour [3]. Liu et al. [4] investigated numerically the effect of thermal radiation on the heat transfer characteristics of a viscous liquid film flow past an unsteady stretching sheet. The influence of Cattaneo-Christov mass and heat diffusion on mixed convective of Darcy-Forchheimer viscous liquid flow along an exponentially stretching sheet was studied by Muhammad et al. [5]. Megahed et al. [6] studied the effects of thermal radiation and heat flux on a MHD boundary layer

laminar flow and heat transfer past an unsteady stretching sheet. Later, some researchers have been engaged in recent developments about nanofluids flow past stretching sheet are highlighted in Refs. [7, 8]. Also, there are numerous researchers studied the steady/unsteady fluid flow subject to a stretchable sheets with variables thickness under different categories and conditions [9, 10].

The study of non-Newtonian fluids has attracted many researchers owing to its enormous wide applications in chemical engineering, bio-fluid, foods, rubber, manufacturing and processing industries. The study of non-Newtonian fluid has complicated and difficult to understand for its complex nature, therefore several empirical and semi-empirical models have been developed. For instance, Rosali et al. [11] studied numerically the micropolar fluid flow through a porous medium past stretching sheet. The analytical solutions of convection Casson fluid flow over an oscillating plate with considering slip boundary conditions was investigated by Imran et al. [12]. Ali et al. [13] have discussed the thermal stratification effects at a stagnation point of a Jeffery fluid flow past stretching cylinder through Cattaneo-Christov heat flux model. Shateyi et al. [14] have made numerical analysis on an unsteady free convection boundary layer flow of Williamson fluid over a stretching sheet with heat transfer. Powell-Eyring model is one of the non-Newtonian fluid models which is derived from kinetic theory of gases instead of empirical formula. One of the advantages of Powell-Eyring fluid model, its empirical fundamental capability to illustrate Newtonian behavior for both high and low shear rates [15]. The hydrodynamic Powell-Eyring fluid flow problem was further investigated by Khan et al. [16] over a rotating disk, by Hayat et al. [17] on Cattaneo-Christov heat flux in the flow of Eyring-Powell fluid, by Ali et al. [18] and Nazeer et al. [19, 20] in a pipe and by Alsaedi et al. [21], Muhammad et al. [22] and Patil et al. [23] for nano Powell-Eyring fluid flow. The study of thermal radiation effect has attracted much attention of researchers for its wide applications in many branches of science and Technology such as electric power, food, and solar cell panels. Due to this immense importance, thermal radiation phenomenon were subsequently examined in different aspects by several researchers [24–30].

The previous important studies encouraged us to investigate some other properties of flows of Powell-Eyring fluid which may be interesting from the point of view of practical applications. One of the most significant of these practical applications is the cooling process, which is one of the advantages especially in the presence of thermal stratification phenomenon [31, 32] of this complicated non-Newtonian model. On the other hand, this advantage can decreases the cost of the final product in which it can be the principle factor in avoiding the malfunctioning of the products. It is interesting to refer here that in our present study we concentrate our attention to the influence of viscous dissipation and the variable fluid properties on the flow characteristics which were absent in the previous work of Jabeen et al. [32]. Therefore, the present study has been undertaken and the combined effect of the thermal stratification and the thermal radiation are also taken into consideration. Also, the numerical technique via Chebyshev spectral method in which the solution of the proposed problem is introduced is more fully discussed.

2. Analysis of the problem

We consider the steady state flow of an incompressible Powell-Eyring fluid over a stretching sheet with a velocity $U_w = ax$ in the horizontal direction toward the $x-$ axis. The sheet is assumed to has a temperature $T_w = T_0 + b_1 x$ which is dependent on $x-$ axis. The ambient fluid layer has a temperature

T_∞. The flow configuration and the co-ordinate system are shown in the following Figure 1.

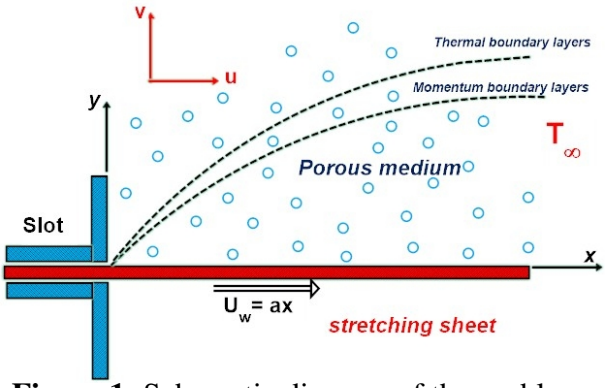

Figure 1. Schematic diagram of the problem.

In our study, we assume that all the physical properties of the fluid are constant except for the viscosity and thermal conductivity. It is assumed that the sheet is being stretched with a linear velocity $u = ax$, where a is the linear stretching rate; x is the distance from the slit. The shear tensor τ_{ij} of Powell Eyring model is given by [33] as follows:

$$\tau_{ij} = \mu\frac{\partial u_i}{\partial x_j} + \frac{1}{\tilde{\beta}}\sinh^{-1}\Big(\frac{1}{C}\frac{\partial u_i}{\partial x_j}\Big), \tag{2.1}$$

where $\tilde{\beta}$ and C are the characteristics of Powell-Eyring Model.

Considering $\sinh^{-1}\Big(\frac{1}{C}\frac{\partial u_i}{\partial x_j}\Big) \cong \frac{1}{C}\frac{\partial u_i}{\partial x_j} - \frac{1}{6}\Big(\frac{1}{C}\frac{\partial u_i}{\partial x_j}\Big)^3, \quad |\frac{1}{C}\frac{\partial u_i}{\partial x_j}| \leq 1.$

Under boundary layer approximation, the continuity, momentum, and energy equations can be written as

$$\frac{\partial u}{\partial x} + \frac{\partial v}{\partial y} = 0, \tag{2.2}$$

$$u\frac{\partial u}{\partial x} + v\frac{\partial u}{\partial y} = \frac{1}{\rho_\infty}\frac{\partial}{\partial y}\Big(\mu\frac{\partial u}{\partial y} + \frac{1}{\tilde{\beta}C}\frac{\partial u}{\partial y} - \frac{1}{6\tilde{\beta}C^3}(\frac{\partial u}{\partial y})^3\Big) - \frac{\mu}{\rho_\infty k}u, \tag{2.3}$$

$$u\frac{\partial T}{\partial x} + v\frac{\partial T}{\partial y} = \frac{1}{\rho_\infty c_p}\frac{\partial}{\partial y}\Big(\kappa\frac{\partial T}{\partial y}\Big) - \frac{1}{\rho_\infty c_p}\frac{\partial q_r}{\partial y} + \frac{1}{\rho_\infty c_p}\Big(\mu(\frac{\partial u}{\partial y})^2 + \frac{1}{\tilde{\beta}C}(\frac{\partial u}{\partial y})^2 - \frac{1}{6\tilde{\beta}C^3}(\frac{\partial u}{\partial y})^4\Big). \tag{2.4}$$

It is interesting to refer here that the last term of the momentum Eq (2.3) confirm the flow of the fluid through a porous medium under the empirical Darcy Law [34, 35]. In this research, the fluid thermal conductivity is assumed to vary as a linear function of temperature, whereas the fluid viscosity is assumed to vary exponentially of temperature [6] as :

$$\kappa = \kappa_\infty(1 + \varepsilon(\frac{T - T_\infty}{T_w - T_0})), \tag{2.5}$$

$$\mu = \mu_\infty e^{-\gamma(\frac{T-T_\infty}{T_w-T_0})}, \tag{2.6}$$

where μ_∞ is the dynamic viscosity away from the sheet, κ_∞ is the thermal conductivity at the ambient, γ is the dimensionless viscosity parameter and ε is the thermal conductivity parameter. The Rosseland approximation [36] for the radiation heat flux q_r is given by :

$$q_r = -\frac{4\sigma^*}{3k^*}\frac{\partial T^4}{\partial y}. \tag{2.7}$$

In our study, we suppose that the temperature differences within the fluid flow are such that the term T^4 may be represented as a linear function of temperature about T_0. Then, expanding T^4 using the Taylor series about T_0 and neglecting higher order terms, so we have [37]:

$$T^4 \cong 4T_0^3 T - 3T_0^4. \tag{2.8}$$

In order to complete the formulation of the proposed problem, it is necessary to provide the appropriate boundary conditions. The appropriate boundary conditions are :

$$u = U_w = ax, \qquad v = 0, \qquad T = T_w = T_0 + b_1 x \quad at \;\; y = 0, \tag{2.9}$$

$$u \to 0, \quad T \to T_\infty = T_0 + b_2 x \quad as \;\; y \to \infty. \tag{2.10}$$

The mathematical analysis of the problem is simplified by introducing the following dimensionless coordinates:

$$\psi = \sqrt{a\nu_\infty} x f(\eta), \qquad \eta = \sqrt{\frac{a}{\nu_\infty}} y, \tag{2.11}$$

$$\theta(\eta) = \frac{T - T_\infty}{T_w - T_0}. \tag{2.12}$$

Equations (2.3), (2.4) and the corresponding boundary conditions (2.9), (2.10) are transformed into the ordinary differential equation with the aid of Eqs (2.11), (2.12). Thus, the governing equations using the dimensionless functions $f(\eta)$ and $\theta(\eta)$ become :

$$f'''\left(e^{-\gamma\theta} + \alpha(1 - \delta f''^2)\right) - \gamma f'' \theta' e^{-\gamma\theta} - f'^2 + f f'' - \lambda e^{-\gamma\theta} f' = 0, \tag{2.13}$$

$$\frac{1}{Pr}\left((1 + R + \varepsilon\theta)\theta'' + \varepsilon\theta'^2\right) + f\theta' - f'\theta - e_1 f' + Ec f''^2\left[(e^{-\gamma\theta} + \alpha) - \frac{\alpha\delta}{3} f''^2\right] = 0, \tag{2.14}$$

$$f(0) = 0, \qquad f'(0) = 1, \qquad \theta(0) = 1 - e_1, \tag{2.15}$$

$$f' \to 0, \quad \theta \to 0, \quad as \quad \eta \to \infty, \tag{2.16}$$

where a prime denotes differentiation with respect to η, α, δ are dimensionless material fluid parameters. It is interesting to observe that if both the material fluid parameters α and δ vanishes (α $=\delta$ $=0$) from Eq (2.13), we reach to a particular case of the Powell-Eyring model which is a Newtonian fluid model. λ is the porous parameter, R is the radiation parameter, e_1 is the thermal stratification parameter, Ec is the Eckert number and Pr is the Prandtl number. The definitions of these parameters are

$$\alpha = \frac{1}{\mu_\infty \tilde{\beta} C}, \quad \delta = \frac{a\rho_\infty U_w^2}{2\mu_\infty C^2}, \quad \lambda = \frac{\nu_\infty}{ak}, \quad R = \frac{16\sigma^* T_0^3}{3\kappa_\infty k^*}, \tag{2.17}$$

$$e_1 = \frac{b_2}{b_1}, \quad Ec = \frac{U_w^2}{c_p(T_w - T_0)}, \quad Pr = \frac{\mu_\infty c_p}{\kappa_\infty}. \tag{2.18}$$

The skin friction coefficient (Cf_x) and local Nusselt number (Nu_x), can be written as

$$Cf_x Re^{\frac{1}{2}} = -\left[(e^{-\gamma\theta(0)} + \alpha) f''(0) - \frac{\alpha\delta}{3} f''^3(0)\right], \quad \frac{Nu_x Re^{\frac{-1}{2}}}{1 + R} = -\theta'(0), \tag{2.19}$$

where $Re = \frac{U_w x}{\nu_\infty}$ is the local Reynolds number.

3. Numerical method for solution

Firstly, we must mention that the Chebyshev spectral method convert the domain of the system (2.13), (2.14) from $[0, \infty]$ to $[-1, 1]$. This mission can be achieved after using the relation $\eta = \frac{\eta_\infty}{2}(\chi+1)$. So, we observe that the new form of the governing Eqs (2.13), (2.14) and their boundary conditions (2.15), (2.16) can be written as:

$$\left[e^{-\gamma\theta}f''' + \alpha\left(1 - \delta\left(\frac{2}{\eta_\infty}\right)^4 f''^2\right)f''' - \gamma e^{-\gamma\theta}f''\theta'\right] - \left(\frac{\eta_\infty}{2}\right)(f'^2 - ff'') + \lambda e^{-\gamma\theta}\left(\frac{\eta_\infty}{2}\right)^2 f' = 0, \tag{3.1}$$

$$(1 + R + \varepsilon\theta)\theta'' + \varepsilon\theta'^2 + Pr(f\theta' - f'\theta - e_1 f')\left(\frac{\eta_\infty}{2}\right) + Ec\left(\frac{2}{\eta_\infty}\right)^2 f''^2 \left[(e^{-\gamma\theta} + \alpha) - \frac{\alpha\delta}{3}\left(\frac{2}{\eta_\infty}\right)^4 f''^2\right] = 0. \tag{3.2}$$

Also, the boundary conditions become:

$$f(\chi) = 0, \qquad f'(\chi) = \frac{\eta_\infty}{2}, \qquad \theta(\chi) = 1 - e_1, \qquad \chi = -1, \tag{3.3}$$

$$f'(\chi) = 0, \qquad \theta(\chi) = 0, \qquad \chi = 1, \tag{3.4}$$

the new functions $f(\chi)$ and $\theta(\chi)$ that appear in Eqs (3.1), (3.2) are unknown functions from $C^m[-1, 1]$, and the differentiation which appear in the same system will be with respect to the new variable χ. Our technique is accomplished by starting with a Chebyshev approximation for the highest order derivatives $f^{(3)}$ and $\theta^{(2)}$ and generating approximations to the lower order derivatives $f^{(i)}$, $i = 0, 1, 2$ and $\theta^{(i)}$, $i = 0, 1$ as follows:
Setting $f^{(3)}(\chi) = \phi(\chi)$ and $\theta^{(2)}(\chi) = \xi(\chi)$, then by integration we obtain $f^{(2)}(\chi)$, $f^{(1)}(\chi)$, $f(\chi)$, $\theta^{(1)}(\chi)$ and $\theta(\chi)$ as follows:

$$\begin{aligned} f^{(2)}(\chi) &= \int_{-1}^{\chi}\phi(\chi)d\chi + c_0, \\ f^{(1)}(\chi) &= \int_{-1}^{\chi}\int_{-1}^{\chi}\phi(\chi)d\chi d\chi + (\chi+1)c_0 + c_1, \\ f(\chi) &= \int_{-1}^{\chi}\int_{-1}^{\chi}\int_{-1}^{\chi}\phi(\chi)d\chi d\chi d\chi + \frac{(\chi+1)^2}{2!}c_0 + \frac{(\chi+1)}{1!}c_1 + c_2, \end{aligned} \tag{3.5}$$

$$\begin{aligned} \theta^{(1)}(\chi) &= \int_{-1}^{\chi}\xi(\chi) + d_0, \\ \theta(\chi) &= \int_{-1}^{\chi}\int_{-1}^{\chi}\xi(\chi)d\chi d\chi + (\chi+1)d_0 + d_1. \end{aligned} \tag{3.6}$$

Here, the constants of integration c_i, d_i, $i = 0, 1, 2$, can be obtained from the outer boundary condition (3.4) as follows:

$$c_0 = -\frac{1}{4}\left(\eta_\infty + 2\int_{-1}^{1}\int_{-1}^{\chi}\phi(\chi)d\chi d\chi\right), \qquad c_1 = \frac{\eta_\infty}{2}, \qquad c_2 = 0,$$

$$d_0 = \frac{1}{2}\left(e_1 - 1 - \int_{-1}^{1}\int_{-1}^{\chi} \xi(\chi) d\chi d\chi\right), \qquad d_1 = -(e_1 - 1).$$

Therefore, we can give approximations to Eqs (3.1), (3.2) as follows:

$$\begin{aligned} f_i &= \sum_{j=0}^{n} \ell_{ij}^{f} \phi_j + c_i^{f}, \qquad f_i^{(1)} = \sum_{j=0}^{n} \ell_{ij}^{f1} \phi_j + c_i^{f1}, \qquad f_i^{(2)} = \sum_{j=0}^{n} \ell_{ij}^{f2} \phi_j + c_i^{f2}, \\ \theta_i &= \sum_{j=0}^{n} \ell_{ij}^{\theta} \xi_j + d_i^{\theta}, \qquad \theta_i^{(1)} = \sum_{j=0}^{n} \ell_{ij}^{\theta 1} \xi_j + d_i^{\theta 1}, \end{aligned} \tag{3.7}$$

for all $i = 0, 1, 2, ..., n$, where

$$\begin{aligned} &\ell_{ij}^{f} = b_{ij}^{3} - \frac{1}{4}(\chi_i + 1)^2 b_{nj}^{2}, \qquad \ell_{ij}^{f1} = b_{ij}^{2} - \frac{1}{2}(\chi_i + 1) b_{nj}^{2}, \qquad \ell_{ij}^{f2} = b_{ij} - \frac{1}{2} b_{nj}^{2}, \\ &\ell_{ij}^{\theta} = b_{ij}^{2} - \frac{1}{2}(\chi_i + 1) b_{nj}^{2}, \qquad \ell_{ij}^{\theta 1} = b_{ij} - \frac{1}{2} b_{nj}^{2}, \\ &c_i^{f} = -\frac{\eta_\infty}{8}\left((\chi_i + 1)^2 - 4(\chi_i + 1)\right), \qquad c_i^{f1} = -\frac{\eta_\infty}{4}(\chi_i - 1), \qquad c_i^{f2} = -\frac{\eta_\infty}{4}, \\ &d_i^{\theta} = \frac{(e_1 - 1)(\chi_i + 1)}{2} - e_1 + 1, \qquad d_i^{\theta 1} = \frac{(e_1 - 1)}{2}, \end{aligned}$$

where $b_{ij}^{2} = (\chi_i - \chi_j) b_{ij}$, $b_{ij}^{3} = \frac{(\chi_i - \chi_j)^2}{2!} b_{ij}$, and b_{ij} are the elements of the matrix B as given in Ref. [39]. By using Eq (3.7), one can transform Eqs (3.1), (3.2) to the following system of non-linear equations in the highest derivative:

$$\begin{aligned} \phi_i \left[e^{-\gamma\theta_i} + \alpha\left(1 - \delta\left(\frac{2}{\eta_\infty}\right)^4 (f_i^{(2)})^2\right)\right] - \gamma e^{-\gamma\theta_i} f_i^{(2)} \theta_i^{(1)} - \left(\frac{\eta_\infty}{2}\right)((f_i^{(1)})^2 - f_i f_i^{(2)}) + \\ \lambda e^{-\gamma\theta_i}\left(\frac{\eta_\infty}{2}\right)^2 f_i^{(1)} = 0, \end{aligned} \tag{3.8}$$

$$\begin{aligned} (1 + R + \varepsilon\theta_i)\,\xi_i + \varepsilon(\theta_i^{(1)})^2 + Pr\left(\frac{\eta_\infty}{2}\right)\left(f_i\theta_i^{(1)} - \theta_i f_i^{(1)} - e_1 f_i^{(1)}\right) + Ec\left(\frac{2}{\eta_\infty}\right)^2 (f_i^{(2)})^2 \\ \left[(e^{-\gamma\theta_i} + \alpha) - \frac{\alpha\delta}{3}\left(\frac{2}{\eta_\infty}\right)^4 (f_i^{(2)})^2\right] = 0, \\ i = 0, 1, ..., n. \end{aligned} \tag{3.9}$$

The last system can be described as a $2n+2$ non-linear algebraic equations. Also, both the unknowns ϕ_i and ξ_i, for $(i = 0, 1, ..., n)$ can be solved using Newton's iteration technique. After solving this system and substitute ϕ_i and ξ_i in Eq (3.7), we can obtain the numerical solution of the system of Eqs (2.13), (2.14).

4. Validation of the Chebyshev spectral method

To validate the accuracy and the efficiency of the numerical procedure used here through the Chebyshev spectral method, computations for the values of the skin-friction coefficient in terms of $-f''(0)$ are carried out for viscous fluid for various values of dimensionless material fluid parameters α and δ. The resulted data are compared with the available published results of Hayat et al. [38] who utilized three different techniques namely Homotopy analysis method, shooting method and bvp4c for the skin-friction as shown in Table 1. From our observation for the tabular data which appear in Table 1, favorable agreement has been obtained with our results. So, this comparison confirms the reliability of the Chebyshev spectral method.

Table 1. Comparison of present values of $-f''(0)$ with values obtained by Hayat et al. [38] for various values of material fluid parameters α and δ with $\gamma = \lambda = 0$.

α	δ	Hayat et al. [38]	Present work
0.1	0.1	0.956017	0.95601695
0.2	0.1	0.917970	0.91796980
0.3	0.1	0.883224	0.88322379
0.1	0.1	0.956017	0.95601695
0.1	0.5	0.964862	0.96486289
0.1	1.0	0.975312	0.97531099

5. Results and discussion

The investigation of the effects of viscous dissipation, thermal radiation and the variation of electrical conductivity on the flow characteristics of non-Newtonian Powell-Eyring fluids carried out in the preceding paragraphs enable us to reach to the present section. The system of equations that governing our physical problem is solved numerically by Chebyshev spectral method because it achieve highly accuracies more than other numerical methods. Figure 2a, b depict the variation of velocity and temperature; respectively with α parameter. It is clear from the figures that the velocity increases with increase in α parameter; while the reverse trend is noted for the temperature distribution. The increase in α parameter corresponds to decrease in the Powell-Eyring fluid viscosity μ_∞ for fixed fluid characteristics $\tilde{\beta}$ and C. Thus the fluid viscosity affects both the flow and heat transfer fields. Physically, It is tentatively suggested here, that the increase of the velocity field or the decrease in the temperature field could be brought about by choosing a non-Newtonian Powell-Eyring fluid which having a great α parameter.

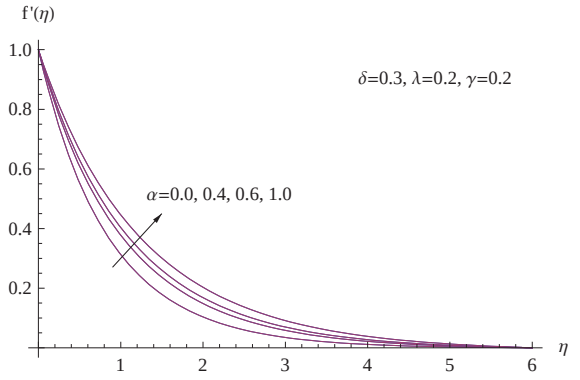

Figure 2. (a) $f'(\eta)$ for assorted values of α.

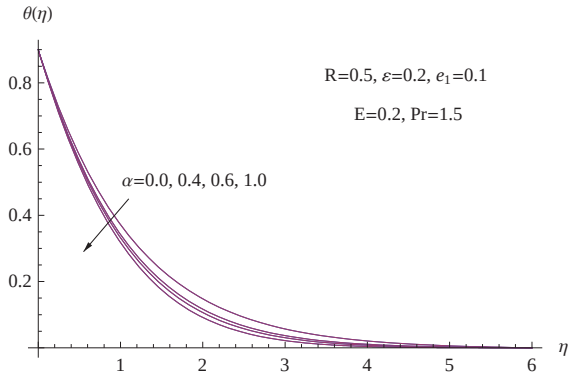

(b) $\theta(\eta)$ for assorted values of α.

In order to see the influence of the δ parameter, both the velocity and the temperature distributions are plotted against δ in the following Figure 3a, b. The Figure 3a shows that with increasing δ, the velocity slightly decreases. Additional insight into the influence of the same parameter on the temperature field can be observed from Figure 3b. This figure reveals that a slightly increase in temperature distribution may be occur with increasing δ.

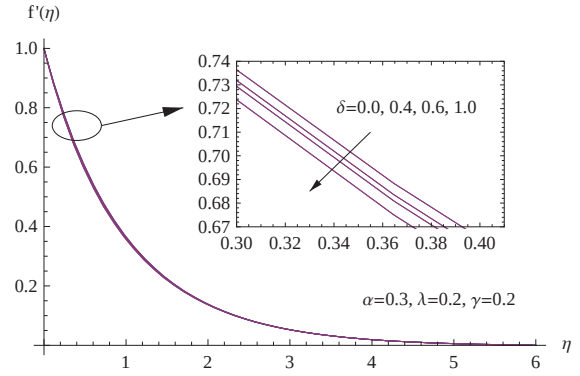

Figure 3. (a) $f'(\eta)$ for assorted values of δ.

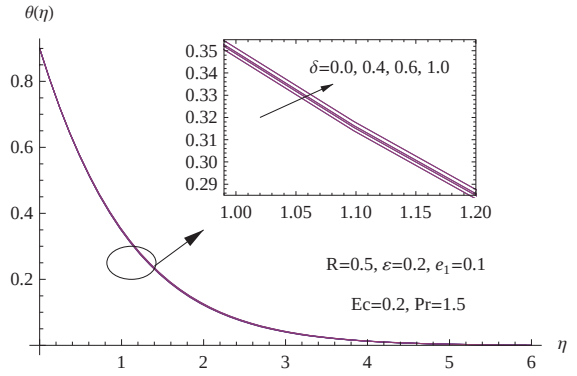

(b) $\theta(\eta)$ for assorted values of δ.

The variation of velocity and temperature with viscosity parameter γ has been displayed in the Figure 4a, b. It is observed that the velocity decreases with increase in the viscosity parameter γ while the temperature slightly increases with increase in the same parameter γ. Thus temperature can be controlled by choosing an appropriate value for the viscosity parameter γ. This type of situation arises in polymer technology, where the sheets moves in the quiescent fluids and the temperature of the fluid has to be controlled so that the sheets are not spoiled due to unnecessary and sudden rise in temperature. Likewise, a correlation of the fluid viscosity with temperature which directly affected the velocity field was the reason to a very sensitive small changes in temperature field.

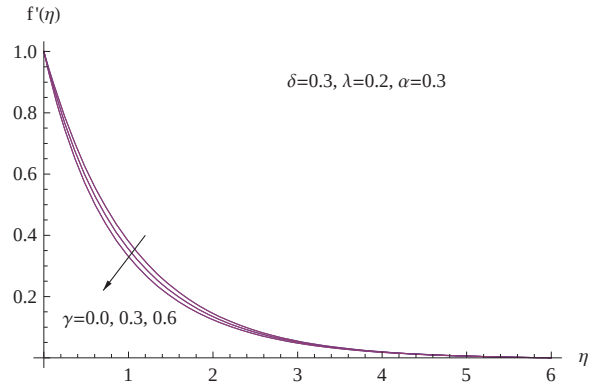

(a) $f'(\eta)$ for assorted values of γ.

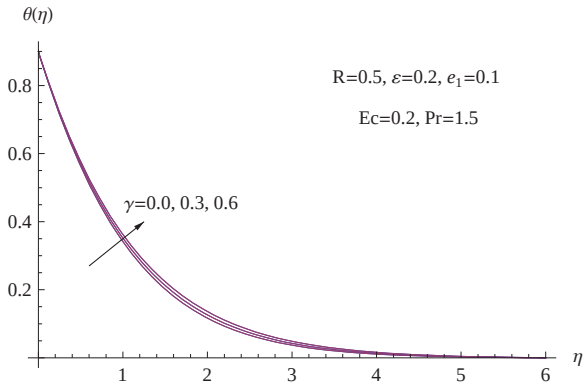

(b) $\theta(\eta)$ for assorted values of γ.

Figure 4.

Figure 5a, b illustrates the variation of velocity $f'(\eta)$ and temperature $\theta(\eta)$ profiles with η over a range of the porous parameter λ. These figures clearly shows that the velocity profiles decrease with the increase in the value of λ. However, as seen from Figure 5b, heat distribution is a weak function of λ and exhibits slight changes through the thermal boundary layer. Therefore, the slightly thickening of the thermal boundary layer occurs with the increase of λ. It is suggested physically that the results will provide a guide to weaken the velocity field as is the case in a fluid flow through a porous medium having great λ parameter.

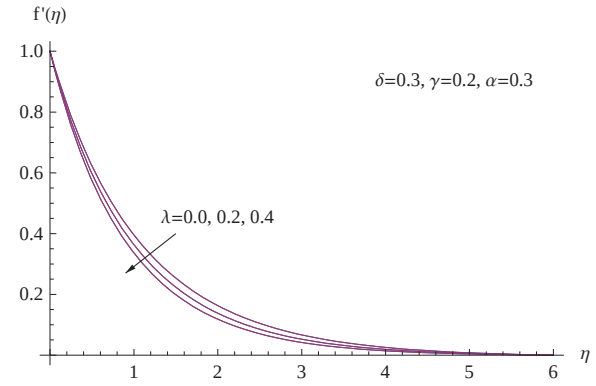

(a) $f'(\eta)$ for assorted values of λ.

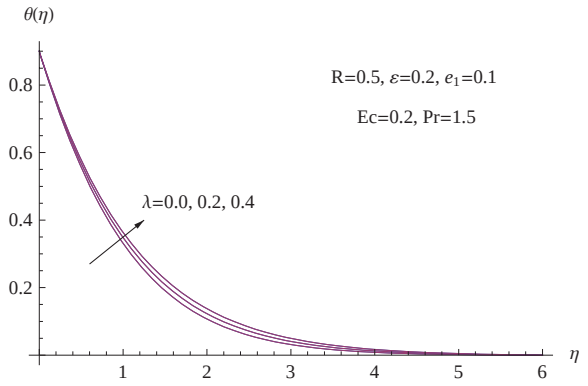

(b) $\theta(\eta)$ for assorted values of λ.

Figure 5.

Figure 6a, b display the velocity distribution and the temperature distribution with the radiation parameter R respectively. From Figure 6a, b it is observed that the velocity slightly increases with increase in the radiation parameter. However, a similar trend is observed for the temperature profiles as presented in Figure 6b, where greater boundary layer thickness and greater temperature distribution imply the presence of larger thermal radiation at the surface. Such type phenomenon occurs in many chemical process where are need to change or faster the velocity of fluid and controlling the heat transfer rate after effecting with the thermal radiation phenomenon.

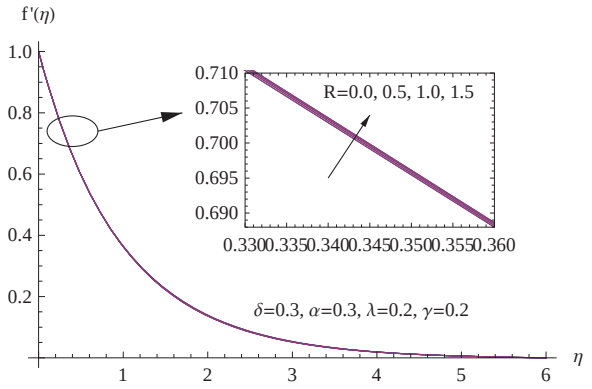

Figure 6. (a) $f'(\eta)$ for assorted values of R.

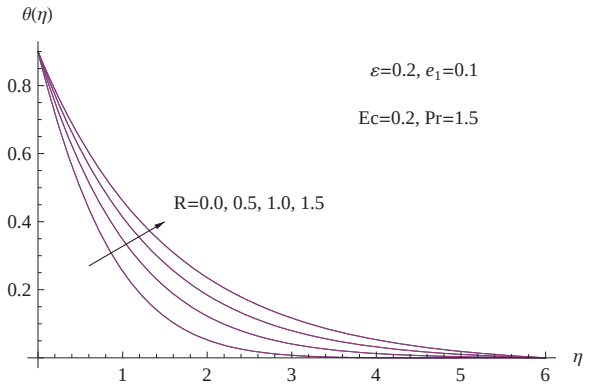

(b) $\theta(\eta)$ for assorted values of R.

Since the constant value usually chosen for the thermal conductivity ε is not realistic, the conductivity varies under the actual conditions of flow in a boundary layer. This will change the skin friction and heat transfer from that found with the constant conductivity. So, from this truth, Figure 7a, b show that increasing ε results in a slightly increase in the velocity field. Also, it is noticed from Figure 7b that a noticeable increase in the thermal boundary layer thickness, associated with an increase in the wall temperature gradient, and hence produces an increase in the surface heat transfer rate with an increase in ε parameter. Physically, the reason for the greatest effect of thermal conductivity parameter ε on the thermal field than the velocity field is the direct existence of this parameter in the energy equation while it indirectly affect the velocity field.

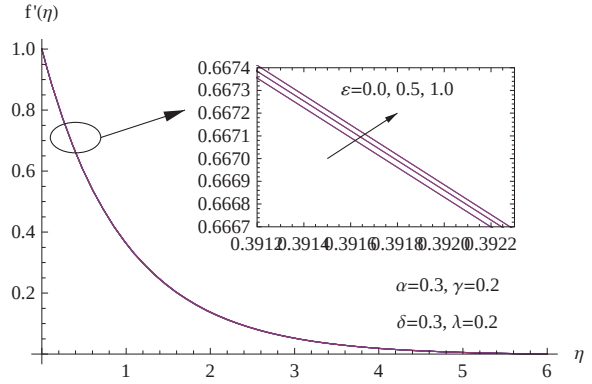

Figure 7. (a) $f'(\eta)$ for assorted values of ε.

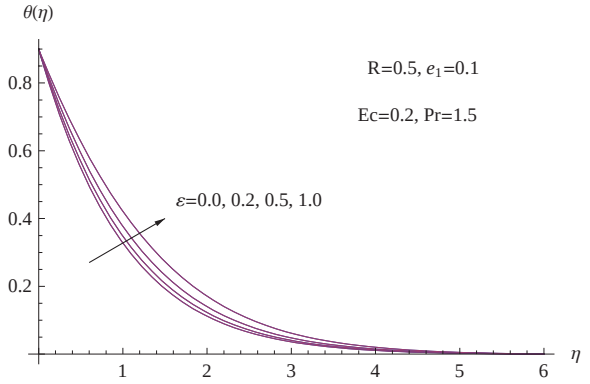

(b) $\theta(\eta)$ for assorted values of ε.

The samples of velocity and temperature profiles for different values of Eckert number Ec are presented in Figure 8a, b respectively when the other parameters are fixed. From these figures, it is seen that the boundary conditions (15), (16) are satisfied. Moreover, it is observed that the velocity profiles slightly increases when Ec increases. This is because, when Ec increases, the stretching velocity U_w increases and slightly speed up the flow, hence reduces the skin friction. On the other hand, from Figure 8b it is observed that the temperature field is strongly influenced by dissipation mechanism due to the increased importance of viscous dissipation phenomenon in faster heat flow. Physically, viscous dissipation is a direct function of the velocity gradient, it would be expected that the influence of this phenomenon would be the greatest on the temperature field due to the direct presence of the dissipation term in the energy equation.

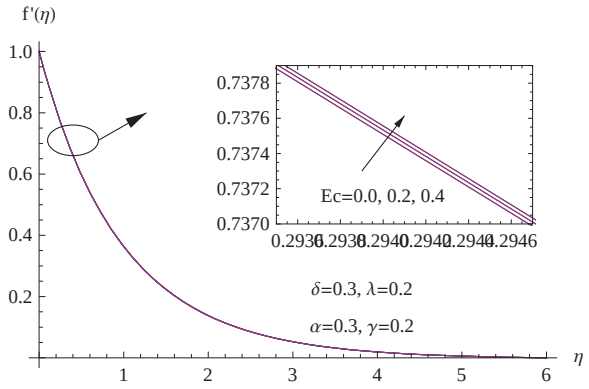

Figure 8. (a) $f'(\eta)$ for assorted values of Ec.

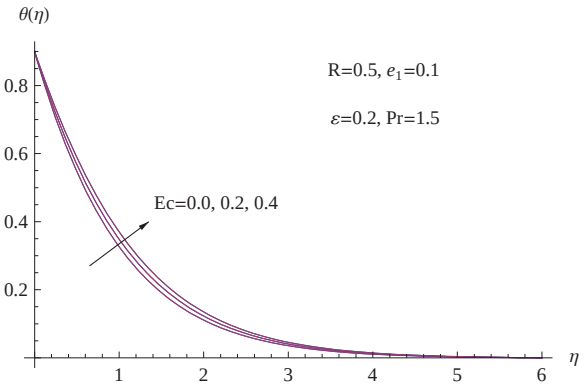

(b) $\theta(\eta)$ for assorted values of Ec.

Figure 9a, b shows the velocity $f'(\eta)$ and temperature $\theta(\eta)$ variations as functions of the space coordinate η for various values of the thermal stratification parameter e_1. As noticed, the thermal stratification parameter e_1 has a slightly effect on the velocity field in comparison with results given for the heating field. For relatively high sheet temperature $\theta(0)$ the primary mechanism for this mission was small thermal stratification parameter e_1. Quite surprisingly, the results presented in Figure 9b, physically means that the great stratification parameter e_1 can be basically adopted as a dominate parameter of the cooling process for the sheet surface.

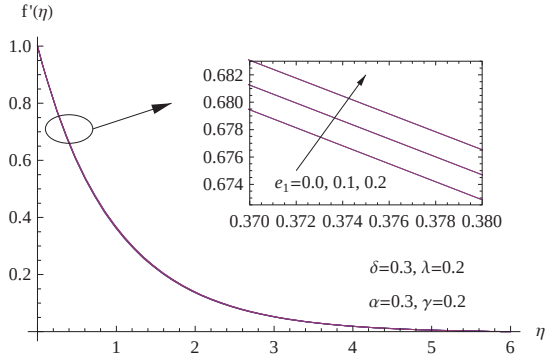

Figure 9. (a) $f'(\eta)$ for assorted values of e_1.

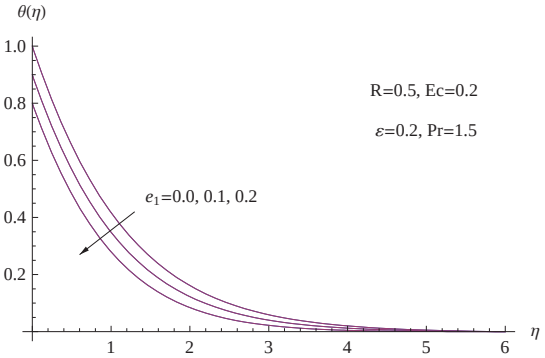

(b) $\theta(\eta)$ for assorted values of e_1.

The effect of governing parameters on the skin-friction coefficient $Cf_x(Re_x)^{\frac{1}{2}}$ and the heat transfer coefficient $\frac{Nu_x(Re_x)^{\frac{-1}{2}}}{1+R}$ has been presented in the following Table 2. From these tabular date, we observe that both the skin-friction coefficient and the local Nusselt number decreases monotonically with increase in both the material parameter δ and the viscosity parameter γ. Further it is observed that the effect of Eckert number and the variable thermal conductivity parameter is to decrease the local Nusselt number. Similar effect is observed by increasing the stratification parameter e_1 on the local Nusselt number. In addition, the effect of increasing values of porous parameter λ is to enhance the skin-friction coefficient whereas its effect is to decrease the local Nusselt number.

Table 2. Values for $Cf_x(Re_x)^{\frac{1}{2}}$ and $\frac{Nu_x(Re_x)^{\frac{-1}{2}}}{1+R}$ for different values of α, δ, ε, γ, R, Ec, e_1 and λ with $Pr = 1.5$ using Chebyshev spectral method.

α	δ	γ	λ	R	ε	Ec	e_1	$Cf_x(Re_x)^{\frac{1}{2}}$	$\frac{Nu_x(Re_x)^{\frac{-1}{2}}}{1+R}$
0.0	0.3	0.2	0.2	0.5	0.2	0.2	0.1	0.991721	0.514780
0.4	0.3	0.2	0.2	0.5	0.2	0.2	0.1	1.199541	0.539417
0.6	0.3	0.2	0.2	0.5	0.2	0.2	0.1	1.293230	0.547907
1.0	0.3	0.2	0.2	0.5	0.2	0.2	0.1	1.464872	0.560372
0.3	0.0	0.2	0.2	0.5	0.2	0.2	0.1	1.160271	0.535783
0.3	0.4	0.2	0.2	0.5	0.2	0.2	0.1	1.146860	0.533877
0.3	0.6	0.2	0.2	0.5	0.2	0.2	0.1	1.139611	0.532822
0.3	1.0	0.2	0.2	0.5	0.2	0.2	0.1	1.123642	0.530463
0.3	0.3	0.0	0.2	0.5	0.2	0.2	0.1	1.241691	0.541182
0.3	0.3	0.3	0.2	0.5	0.2	0.2	0.1	1.107940	0.530951
0.3	0.3	0.6	0.2	0.5	0.2	0.2	0.1	0.993022	0.520605
0.3	0.3	0.2	0.0	0.5	0.2	0.2	0.1	1.062720	0.554028
0.3	0.3	0.2	0.2	0.5	0.2	0.2	0.1	1.150341	0.534379
0.3	0.3	0.2	0.4	0.5	0.2	0.2	0.1	1.230490	0.516348
0.3	0.3	0.2	0.2	0.0	0.2	0.2	0.1	1.155120	0.987958
0.3	0.3	0.2	0.2	0.5	0.2	0.2	0.1	1.150341	0.534379
0.3	0.3	0.2	0.2	1.0	0.2	0.2	0.1	1.147120	0.341255
0.3	0.3	0.2	0.2	1.5	0.2	0.2	0.1	1.144771	0.239839
0.3	0.3	0.2	0.2	0.5	0.0	0.2	0.1	1.151610	0.580203
0.3	0.3	0.2	0.2	0.5	0.2	0.2	0.1	1.150341	0.534379
0.3	0.3	0.2	0.2	0.5	0.5	0.2	0.1	1.148672	0.479961
0.3	0.3	0.2	0.2	0.5	1.0	0.2	0.1	1.146321	0.413737
0.3	0.3	0.2	0.2	0.5	0.2	0.0	0.1	1.152670	0.587352
0.3	0.3	0.2	0.2	0.5	0.2	0.2	0.1	1.150341	0.534379
0.3	0.3	0.2	0.2	0.5	0.2	0.4	0.1	1.148930	0.481538
0.3	0.3	0.2	0.2	0.5	0.2	0.2	0.0	1.158460	0.552285
0.3	0.3	0.2	0.2	0.5	0.2	0.2	0.1	1.150341	0.534379
0.3	0.3	0.2	0.2	0.5	0.2	0.2	0.2	1.142232	0.516256

6. Conclusions

Our aim at the outset was to obtain proactive data on the thermal properties of non-Newtonian Powell-Eyring model. Four novel contributions are there in our current work. Firstly, both the viscosity and the thermal conductivity of the Powell-Eyring fluid are assumed to alter with temperature through the flow in porous medium. Secondly, the heat transfer mechanism is affected by the thermal radiation along with the thermal stratification phenomenon. Thirdly, energy equation is also influenced with viscous dissipation. Fourthly, we employed Chebyshev spectral method to get the numerical solution of the highly non-linear equations which govern the problem. Based on the outlined numerical solution of the hydrodynamic problem under consideration, the cooling process

has been developed after studying the novel effect of some physical parameters. It is shown that for all physically reasonable boundary conditions employed in the present work, the study predicts the result that a fluid will undergo a great thermal energy when subjected to a simultaneously effect of both thermal radiation and viscous dissipation phenomenon. The important findings of the graphical analysis of the results of the present problem are as follows:

1. We can control cooling process considerably by increasing the thermal stratification parameter.
2. The effect of increasing the values of viscosity parameter, porous parameter, thermal conductivity parameter and the radiation parameter are to enhance the temperature distribution in the flow region.
3. Thermal stratification parameter has another important influence in so far as it can establish a thinner thermal layer.
4. The effect of increasing both values of porous parameter and the viscosity parameter are to decrease the velocity distribution throughout the region of the boundary layer.

Acknowledgments

The authors are thankful to the honorable editor and anonymous reviewers for their useful suggestions and comments which improved the quality of this paper.

Conflict of interests

The authors declare that they have no competing interests.

References

1. L. J. Crane, Flow past a stretching plate, *Z. Angew. Math. Phys.*, **21** (1970), 645–647.
2. C. H. Chen, Laminar mixed convection adjacent to vertical, continuously stretching sheets, *Heat Mass Transfer*, **33** (1998), 471–476.
3. A. J. Chamkha, A. M. Aly, M. A. Mansour, Similarity solution for unsteady heat and mass transfer from a stretching surface embedded in a porous medium with suction/injection and chemical reaction effects, *Chem. Eng. Commun.*, **197** (2010), 846–858.
4. I. C. Liu, A. M. Megahed, Hung-Hsun Wang, Heat transfer in a liquid film due to an unsteady stretching surface with variable heat flux, *J. Appl. Mech.*, **80** (2013), 041003.
5. T. Muhammad, K. Rafique, M. Asma, M. Alghamdi, Darcy-Forchheimer flow over an exponentially stretching curved surface with Cattaneo-Christov double diffusion, *Physica A*, **556** (2020), 123968.
6. A. M. Megahed, M. R. Gnaneswara, W. Abbas, Modeling of MHD fluid flow over an unsteady stretching sheet with thermal radiation, variable fluid properties and heat flux, *Math. Comput. Simul.*, **185** (2021), 583–593.
7. P. M. Patil, M. Kulkarni, P. S. Hiremath, Effects of surface roughness on mixed convective nanofluid flow past an exponentially stretching permeable surface, *Chinese J. Phys.*, **64** (2020), 203–218.

8. N. S. Khashiie, N. M. Arifin, I. Pop, R. Nazar, E. H. Hafidzuddin, N. Wahi, Three-dimensional hybrid nanofluid flow and heat transfer past a permeable stretching/shrinking sheet with velocity slip and convective condition, *Chinese J. Phys.*, **66** (2020), 157–171.
9. D. Pal, D. Chatterjee, K. Vajravelu, Influence of magneto-thermo radiation on heat transfer of a thin nanofluid film with non-uniform heat source/sink, *Propuls. Power Res.*, **9** (2020), 169–180.
10. W. Abbas, A. M. Megahed, Numerical solution for chemical reaction and viscous dissipation phenomena on non-Newtonian MHD fluid flow and heat mass transfer due to a nonuniform stretching sheet with thermal radiation, *Int. J. Mod. Phys. C*, **32** (2021), 2150124.
11. H. Rosali, A. Ishak, I. Pop, Micropolar fluid flow towards a stretching/shrinking sheet in a porous medium with suction, *Int. Commun. Heat Mass Transfer*, **39** (2012), 826–829.
12. I. A. Muhammad, S. Sarwar, M. Imran, Effects of slip on free convection flow of Casson fluid over an oscillating vertical plate, *Bound. Value Probl.*, **2016** (2016), 1–11.
13. A. Usman, K. U. Rehman, M. Y. Malik, Thermal energy statistics for Jeffery fluid flow regime: A generalized Fourier's law outcomes, *Physica A*, **542** (2020), 123428.
14. S. Shateyi, H. Muzara, On the numerical analysis of unsteady MHD boundary layer flow of Williamson fluid over a stretching sheet and heat and mass transfers, *Comput.*, **8** (2020), 55.
15. T. Hayat, Z. Iqbal, M. Qasim, S. Obaidat, Steady flow of an Eyring Powell fluid over a moving surface with convective boundary conditions, *Int. J. Heat Mass Tran.*, **55** (2012), 1817–1822.
16. N. A. Khan, S. Aziz, N. A. Khan, MHD flow of Powell-Eyring fluid over a rotating disk, *J. Taiwan Inst. Chem. Eng.*, **45** (2014), 2859–2867.
17. T. Hayat, M. I. Khan, M. Waqas, A. Alsaedi, On Cattaneo-Christov heat flux in the flow of variable thermal conductivity Eyring-Powell fluid, *Results Phys.*, **7** (2017), 446–450.
18. N. Ali, F. Nazeer, M. Nazeer, Flow and heat transfer of Eyring-powell fluid in a pipe, *Z. Naturforsch. A*, **73** (2018), 265–274.
19. M. Nazeer, F. Ahmad, A. Saleem, M. Saeed, S. Naveed, M. Shaheen, et al., Effects of constant and space dependent viscosity on Eyring-Powell fluid in a pipe: Comparison of perturbation and explicit finite difference method, *Z. Naturforsch. A*, **74** (2019), 961–969.
20. M. Nazeer, F. Ahmad, M. Saeed, A. Saleem, S. Naveed, Z. Akram, Numerical solution for flow of a Eyring-powell fluid in a pipe with prescribed surface temperature, *J. Braz. Soc. Mech. Sci.*, **41** (2019), 518.
21. A. Alsaedi, T. Hayat, S. Qayyum, R. Yaqoob, Eyring-Powell nanofluid flow with nonlinear mixed convection: Entropy generation minimization, *Comput. Meth. Prog. Bio.*, **186** (2020), 105183.
22. T. Muhammad, H. Waqas, S. A. Khan, R. Ellahi, S. M. Sait, Significance of nonlinear thermal radiation in 3D Eyring-Powell nanofluid flow with Arrhenius activation energy, *J. Therm. Anal. Calorim.*, **143** (2021), 929–944.
23. V. S. Patil, A. B. Patil, S. Ganesh, P. H. Pooja, N. S. Patil, Unsteady MHD flow of a nano powell-eyring fluid near stagnation point past a convectively heated stretching sheet in the existence of chemical reaction with thermal radiation, *Mater. Today: Proc.*, **44** (2021), 3767–3776.
24. M. Hamid, T. Zubair, M. Usman, R. U. Haq, Numerical investigation of fractional-order unsteady natural convective radiating flow of nanofluid in a vertical channel, *AIMS Math.*, **4** (2019), 1416–1429.

25. W. Abbas, M. M. Magdy, Heat and mass transfer analysis of nanofluid flow based on, and over a moving rotating plate and impact of various nanoparticle shapes, *Math. Probl. Eng.*, **2020** (2020), Article ID 9606382, 12 pages.
26. W. Abbas, A. S. Emad, Hall current and joule heating effects on free convection flow of a nanofluid over a vertical cone in presence of thermal radiation, *Therm. Sci.*, **21** (2017), 2609–2620.
27. S. S. Ghadikolaei, K. H. Hosseinzadeh, D. D. Ganji, B. Jafari, Nonlinear thermal radiation effect on magneto Casson nanofluid flow with Joule heating effect over an inclined porous stretching sheet, *Case Stud. Therm. Eng.*, **12** (2018), 176–187.
28. E. O. Fatunmbi, A. Adeniyan, Nonlinear thermal radiation and entropy generation on steady flow of magneto-micropolar fluid passing a stretchable sheet with variable properties, *Results Eng.*, **6** (2020), 100142.
29. W. Abbas, K. S. Mekheimer, M. M. Ghazy, A. M. A. Moawad, Thermal radiation effects on oscillatory squeeze flow with a particle-fluid suspension, *Heat Transfer*, **50** (2021), 2129–2149.
30. T. Muhammad, H. Waqas, U. Farooq, M. S. Alqarni, Numerical simulation for melting heat transport in nanofluids due to quadratic stretching plate with nonlinear thermal radiation, *Case Stud. Therm. Eng.*, **27** (2021), 101300.
31. M. Bilal, S. Ashbar, Flow and heat transfer analysis of Eyring-Powell fluid over stratified sheet with mixed convection, *JOEMS*, **28** (2020), 40.
32. I. Jabeen, M. Farooq, M. Rizwan, R. Ullah, S. Ahmad, Analysis of nonlinear stratified convective flow of Powell-Eyring fluid: Application of modern diffusion, *Adv. Mech. Eng.*, **12** (2020), 1–10.
33. R. E. Powell, H. Eyring, Mechanism for relaxation theory of viscosity, *Nature*, **154** (1944), 427–428.
34. N. A. Khan, S. Khan, A. Arab, Flow of micropolar fluid over an off centered rotating disk with modified Darcy's law, *Propuls. Power Res.*, **6** (2017), 285–295.
35. N. A. Khan, F. Naz, F. Sultan, Entropy generation analysis and effects of slip conditions on micropolar fluid flow due to a rotating disk, *Open Eng.*, **7** (2017), 185–198.
36. A. Raptis, C. Perdikis, H. S. Takhar, Effect of thermal radiation on MHD flow, *Appl. Math. Comput.*, **153** (2004), 645–649.
37. A. Raptis, Radiation and viscoelastic flow, *Int. Commun. Heat Mass*, **26** (1999), 889–895.
38. T. Hayat, S. Ali, M. A. Farooq, A. Alsaedi, On comparison of series and numerical solutions for flow of Eyring-Powell fluid with newtonian heating and internal heat generation/absorption, *PLOS ONE*, **10** (2015), 1–13.
39. S. E. El-Gendi, Chebyshev solution of differential, integral and integro-differential equations, *Comput. J.*, **12** (1969), 282–287.